Research article

Investigation of Azo-COP-2 as a photo-responsive low-energy CO_2 adsorbent and porous filler in mixed matrix membranes for CO_2/N_2 separation

Siyao Li[†,a], Nicholaus Prasetya[†,a], and Bradley P. Ladewig[*a,b]

[a]Barrer Centre, Department of Chemical Engineering, Imperial College London, London SW7 2AZ, United Kingdom

[b]Institute for Micro Process Engineering (IMVT), Karlsruhe Institute of Technology, Hermann-von-Helmholtz-Platz 1, 76344 Eggenstein-Leopoldshafen, Germany

[†]Equal contribution

*Corresponding author: bradley.ladewig@kit.edu

Abstract

Azo-COP-2 is a nanoporous polymer with exceptional CO_2/N_2 separation performance. In this study, we further investigate the application of Azo-COP-2 as a low-energy CO_2 adsorbent and porous filler in mixed matrix membranes (MMMs) for CO_2/N_2 separation. As an adsorbent, the UV-irradiated Azo-COP-2 showed lower CO_2 uptake than in the non-irradiated state and Azo-COP-2 also exhibited highly efficient CO_2 photoswitching between the two states. Combined with high CO_2/N_2 selectivity, this makes Azo-COP-2 an excellent candidate for low-energy CO_2 capture and release. Azo-COP-2 is also shown to be a beneficial filler in MMMs. For polysulfone-based MMMs, the CO_2 permeability and CO_2/N_2 selectivity could be increased up to 160% and 66.7%, respectively. The strategy shows the great potential of Azo-COP-2 not only for a low-energy CO_2 adsorbent but also to improve the performance of conventional polymeric membranes for CO_2 post-combustion capture.

---

1. Introduction

There is a growing interest recently in the development of microporous materials which, according to IUPAC definition, have the pore size that is below 2 nm.[1] There are a number of different types of recently-developed microporous materials. They can be built through metal-ligand coordination (metal-organic framework, MOF)[2] or through organic covalent bonding such as in covalent organic framework (COF)[3] and polymer of intrinsic microporosity (PIM).[4] The latter is also generally classified as nanoporous polymers.[5] As with MOFs, nanoporous polymers also have large surface areas and can also be functionalized to make them applicable for various applications such as liquid separation[6] gas separation[7] and catalysis.[8] In addition, these materials could be expected to have a better affinity with other organic materials (something often not the case with MOFs) since their frameworks are constructed from organic building blocks. This property is particularly important when attempting to fabricate a composite material such as mixed matrix membranes (MMMs).[9]

In this study, we chose to study an azobenzene-based nanoporous polymer which is called Azo-COP-2 (COP stands for Covalent Organic Polymers). This material has been previously synthesized through a metal-catalyst-free method and reported to have a superior CO_2/N_2 separation performance compared with the rest of the azo-based COPs.[5, 10] To further explore the utilization of this promising COP, in the first part of this

study, we investigated the photo-responsive property of Azo-COP-2 during CO_2 adsorption. This property renders it to be a potential candidate as a low-energy CO_2 adsorbent by utilizing UV light as one of the main sustainable sources during material regeneration as previously observed in azobenzene-based MOF.[11, 12]

Several investigations regarding the photo-responsive property of nanoporous polymers have been conducted. For instance, an anthracene-based COF (Ph-An-COF) has been studied for its potential as a smart material.[13] After irradiation with UV light, changes in the COF luminescence and porosity were observed. Investigations have also been made in the azobenzene-based nanoporous polymers. Various approaches, apart from change in UV-Vis spectra,[14] can then be employed to highlight the impact of azobenzene photo-isomerization to the material property. Liu and co-workers observed this phenomenon through reversible structural deformation induced by photo-isomerization in an azobenzene-based nanoporous polymers after UV light irradiation.[15] The deformed framework could be brought back to its initial condition by heating. Azobenzene photoisomerization has also been proven able to affect the gas adsorption property of nanoporous polymers. A study in a star-shaped azobenzene porous molecular crystal showed the ability of the material to undergo reversible phase change in crystallinity and CO_2 uptake upon UV irradiation and heat treatment.[16] Another investigation has also been made with porous organic polymers (POP) with a pendant azobenzene group called UCBZ.[17] The authors showed that after the irradiation with UV light, the CO_2 uptake of UCBZ could be increased which was due to the isomerization of the azobenzene from *trans* to *cis* state resulting in more pore opening and increase in gas uptake. However, to the best of our knowledge, there has not been any study of the photo-responsive property of nanoporous polymers which are applicable for low-energy CO_2 capture. Through this work we fill this gap and help expand the applications of photo-responsive nanoporous polymers.

As an advanced adsorbent, we also investigated the utilization of Azo-COP-2 as a filler in mixed matrix membranes (MMM). MMMs are prepared from at least two different materials acting as a discrete phase (fillers) and a continuous matrix. MMMs have been proposed as a promising approach to improve gas separation performance in conventional polymeric membranes because of their ability to synergistically combine different materials properties.[18] Up to now, there are a variety of fillers that have been successfully incorporated into different polymeric matrices such as carbon nanotube,[19, 20] graphene oxide,[21] zeolites,[22, 23] MOFs[24-27] and COFs.[28]

Good interaction between the fillers and polymer matrices is required in MMMs so the fillers can improve the gas separation performance of the bare polymeric membrane. Differing from most other fillers, nanoporous polymers are entirely built from organic-organic covalent bonds which have the potential to fulfil this requirement.[17] This property is expected to bring a benefit during MMMs fabrication. This is because they can have better affinity with organic polymers than classical inorganic particles, making it more likely that the two components are compatible.[29] Therefore, the non-selective voids issue usually observed in MMMs could also be minimized. In addition, as stated previously, Azo-COP-2 has also been shown to have a superior CO_2/N_2 separation performance. Our previous studies have also shown the ability of azobenzene-based MOFs to improve the CO_2/N_2 separation performance in MMMs.[30] Thus, improvement in CO_2/N_2 gas separation performance in Azo-COP-2 based MMMs could also be expected which is applicable for post-combustion CO_2 capture.

2. Experimental Section

2.1 Synthesis of tetrakisnitrophenylmethane.

Tetraphenylmethane (1g) was slowly added to 7ml fuming nitric acid at 0°C in a conical flask with vigorous magnetic stirring for about 10 minutes. The solution was then further stirred for another 20 minutes at this condition. This was followed by bringing the solution to ambient temperature and stirred for another 20 minutes before being brought back to the ice bath and stirred for another 20 minutes. A mixture of acetic anhydride (2ml) and acetic acid (4ml) was then added to the previous solution with constant stirring for another 15 minutes. 8ml acetic acid was then poured into the mixture to dilute the reaction mixture. The precipitate was filtered off under vacuum and further washed with acetic acid (10ml). The obtained yellow crude product was around 0.7g. The yield was around 44.2%. The crude product was then recrystallized from tetrahydrofuran (THF) by firstly dissolving the crude product in 40mL of hot THF in a conical flask. Once the THF was brought to room temperature, pure crystals formed at the bottom of the conical flask and the solution was left overnight. The following day, the yellow crystalline product was obtained by filtration under reduced pressure.

2.2 Synthesis of Azo-COP-2.

Azo-COP-2 was synthesized through a metal catalyst-free method that has been previously reported using tetranitrophenyl methane as the starting material.[5] The synthesis procedure is depicted in **Figure 1**.
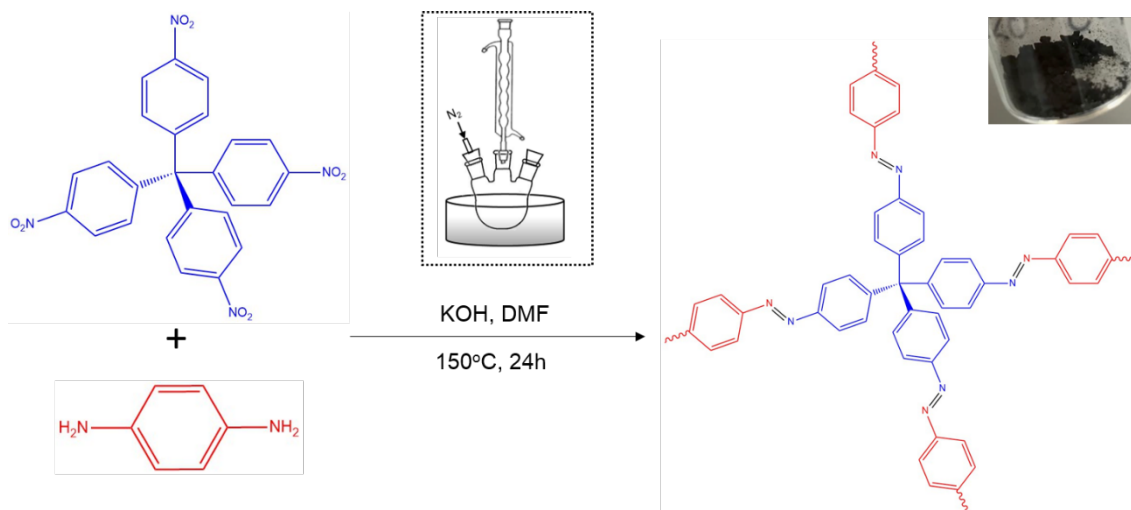
Figure 1. Synthesis route of Azo-COP-2

In brief, tetrakisnitrophenyl methane (0.2g) and p-phenylenediamine (0.086g) were dissolved in DMF (25ml) in a three-necked round flask with strong magnetic stirring. Potassium hydroxide (0.22g) was added to the solution while stirring. The reaction was kept under N_2 atmosphere and the temperature was slowly increased to 150 °C . A reflux condenser was used to condense the vapour during the reaction. The mixture was stirred for 24 hours. The colour of the reaction mixture changed from light yellow to dark purple, which was followed by the formation of brown precipitates. After cooling down to the room temperature, de-ionized water (250 mL) was added to the mixture and it was stirred for half an hour subsequently. The obtained precipitate was then filtered under reduced pressure. Excess de-ionized water, acetone and THF were used to wash the precipitant until the filtrate became clear and colourless. The precipitant was further dried under vacuum at 110 °C overnight. Finally, the brown powder with around 58.9% yield was obtained.

2.3 Fabrication of mixed matrix membranes.

Three different polymers were used in this study: Matrimid, polysulfone and PIM-1. The structures of the polymers are given in **Figure 2**.
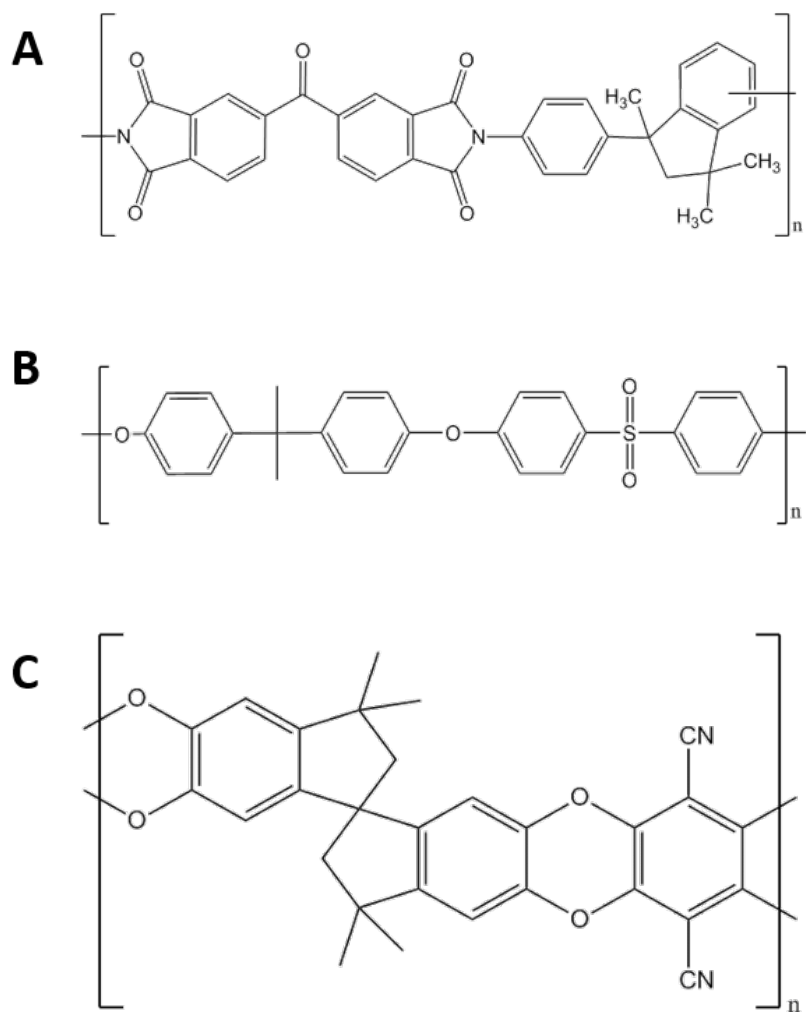
Figure 2. The structure of the polymers used in this study: Matrimid (A), polysulfone (B) and PIM-1 (C)

Matrimid and polysulfone was kindly supplied from Huntsman and BASF, respectively. Meanwhile, PIM-1 was synthesized according to the published procedure.[31] The fabrication processes of mixed matrix membranes are similar regardless of the polymers used. In general, a certain amount of Azo-COP-2 particles were dispersed in THF. About 50 wt% of the polymer was then added into the COF suspension. The solution was then kept stirred overnight to do the priming of Azo-COP-2 with the polymer. Afterwards, the rest of the polymer was added and the final suspension was kept stirred overnight. The obtained homogeneous suspension was then cast on a petri dish covered with perforated aluminium foil. The suspension was left to dry at atmosphere condition in a fume cupboard overnight. This was followed by another 12 hours drying in an oven at 100°C. Three different loadings of MMMs were studied for each polymer: 5, 10 and 15wt%.

Meanwhile, for the pure polymeric membranes, each polymer was directly dissolved in THF which was followed by casting and drying at the same condition as in MMMs.

2.4 Gas permeation testing.

Gas permeation performance of MMMs was evaluated by using the constant-volume variable-pressure method. A complete description of the equipment has been described elsewhere.[32] The membranes were cut from the casted films with certain surface areas and mounted onto the membrane cell. Two pure gas species (CO_2 and N_2) were introduced as testing gases to study their permeabilities through the membranes. During the test, the upstream pressure of both CO_2 and N_2 were maintained at 30psia, 22psia and 14psia for Polysulfone, Matrimid and PIM-1 based MMMs, respectively, considering the strength of membranes. The temperature was kept at 35°C during the whole experiment. The thickness of all membranes and MMMs was measured by using a digital micrometer. For the pure polymeric membranes, the thickness varied in the range of 50 to 70 μm while the thickness of MMMs varied between 80 to 120 μm.

The gas permeability is calculated using equation (1):

$$\text{P} = \frac{273.15 \times 10^{10} \times Vl}{760 \times A \times T \times \left(P_o \times \frac{76}{14.7}\right)} \left(\frac{dp}{dt}\right) \tag{1}$$

Where P is the permeability of gases through membranes in Barrer (1 Barrer = 1×10^{-10} cm^3 (STP) cm/cm^2 s cmHg). l is the thickness of the membranes (cm). V is the constant volume of the designed chamber at permeate side (cm^3). T is the operating temperature (K). A is the effective surface area of membranes (cm^2). P_o is the feed pressure (psia). At steady state, a pressure transmitter was used to measure the increase of downstream pressure in the chamber against time $\left(\frac{dp}{dt}\right)$ (mmHg/s).

Meanwhile, the CO_2/N_2 selectivity (α) is calculated by applying equation (2)

$$\alpha = \frac{P_{CO_2}}{P_{N_2}} \tag{2}$$

A time-lag method was used to evaluate the diffusivity (D) and solubility coefficient (S) of pure CO_2 and N_2 gases through the membranes [25]. The relationship between these two parameters and the membrane permeability is given in Equation (3) while Equation (4) is used to calculate the D value.

$$P = D \times S \tag{3}$$

7

$$D = \frac{l^2}{6\theta} \tag{4}$$

where θ refers to the time lag.

2.5 Various characterization techniques

2.5.1 Powder X-Ray Diffraction (PXRD). PXRD diffractograms were collected using a PANalytical X'Pert Pro diffractometer. During the measurement, 40 kV generator voltage, 20 mA tube current and Cu Kα radiation (λ = 1.54184 Å) at 298 K were used to record the data. The scan step size used in the measurement was 0.016711 2θ degrees and the scan range was from 5 to 70 2θ degree. Powder X-ray diffraction patterns of Azo-COP-2 indicated clearly the formation of amorphous polymer.

2.5.2 Fourier transform infrared spectroscopy (FTIR). The FTIR spectra of the samples were obtained using an Agilent Cary 630 FTIR Spectrometer. The scanning range was set between 4000–650 cm^{-1} with a resolution of 2 cm^{-1}.

2.5.3 Nitrogen sorption analysis. A Micromeritics Tristar instrument was used to collect the N_2 isotherm of Azo-COP-2 at 77 K. Sample mass for each measurement was approximate 50 mg. Prior to the measurement, the Azo-COP-2 particles were degassed at 110 °C overnight.

2.5.4 Azo-COP-2 CO_2 uptake and CO_2 dynamic photo-switching. Both CO_2 uptake and CO_2 dynamic photo-switching of Azo-COP-2 was measured at 273 K and 298 K according to the published procedure.[33, 34] About 50 mg of sample was used in this study. Prior to the measurement, the Azo-COP-2 was degassed overnight under vacuum at 110ºC.

2.5.5 Scanning Electron Microscopy (SEM). The SEM micrographs of gold-sputtered membrane cross-sections were obtained by using a field emission gun scanning electron microscope (FEGSEM) SIGMA 300 operated in secondary electron imaging mode at 20kV accelerating voltage.

3 Results and Discussion

3.1 Characterization and light-responsive property of Azo-COP-2

The successful synthesis of Azo-COP-2 was proven through various characterization techniques such as PXRD, FTIR, N_2 and CO_2 adsorption. These results are presented in **Figure 3**. As can be seen, the PXRD pattern of Azo-COP-2 resembles a formation of an amorphous structure with a broadening peak at around 17°. This is also in agreement with the previously reported result for this material [5]. The FTIR spectrum (**Figure 3 (B)**) confirms the successful synthesis of the Azo-COP-2. Despite the relatively weak FTIR signal that might be caused by the favourable *trans*-state condition of the azo framework in Azo-COP-2,[35] there is a clear indication of the presence of the azobenzene functionality. This could be seen from N=N stretching vibration in azobenzene that gives rise to the FTIR bands located at 1507 and 1467 cm^{-1}. Meanwhile, the peaks at 1608 cm^{-1} corresponds to aromatic C=C and the peak at 1280 cm^{-1} corresponds to the -C-N-bond between the aromatic ring and the azobenzene group.
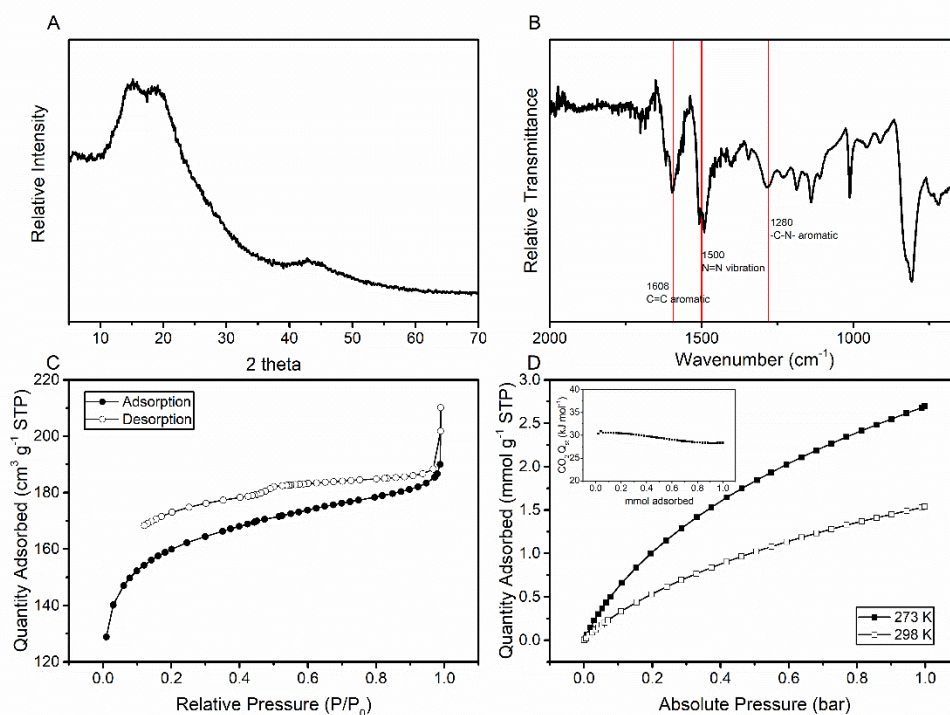
Figure 3. Characterizations of Azo-COP-2: PXRD (A), FTIR (B), N_2 physisorption (C) and CO₂ adsorption (D, inset: CO₂ heat of adsorption)

The porosity of the Azo-COP-2 was also confirmed through gas uptake. Nitrogen physisorption of the Azo-COP-2 was then measured at 77K and the result is presented in **Figure 3 (C).** The typical type-I reversible sorption curves were observed during the measurement showing a steep gas uptake curve at relatively low pressure followed by saturation at higher relative pressure. By applying the Brunauer–Emmet–Teller (BET) model, the surface area (S_{BET}) of Azo-COP-2 was found to be around 554 m^2 g^{-1} and is comparable to the previously reported value (729 m^2 g^{-1})[5] and similar to some emerging COFs, like SNW-1.[28] Meanwhile, the micropore volume was found to be around 0.175 cm^3 g^{-1}. Apart from nitrogen physisorption, the porous structure of Azo-COP-2 was also confirmed through CO_2 uptake study as can be seen in **Figure 3 (D)**. The figure shows the Azo-COP-2 adsorption isotherms of CO_2 at 273 and 298K. The CO_2 adsorption value was found to be around 2.70 and 1.54 mmol g^{-1} at 273 K and 298 K, respectively. As in surface area analysis, the CO_2 uptake of the Azo-COP-2 synthesised in this study was also comparable with the previously reported Azo-COP-2 which was around 2.5 and 1.5 mmol g^{-1} at 273 and 298 K, respectively.[5] The slight difference in surface area and CO_2 uptake of the synthesised Azo-COP-2 in this study might then be caused by some factors such as impurities during materials preparation and trapped moisture during materials activation. Despite this, these results have shown the successful reproduction of Azo-COP-2 used in this study.

Finally, based on the CO_2 uptake data, the CO_2 isosteric heat of adsorption (Q_{st}) was also calculated using the Clausius-Clapeyron equation and the result is presented in the inset of **Figure 3 (D)**. At low coverage, the Q_{st} was found to be around 31.3 kJ mol^{-1} and plateauing at around 28 kJ mol^{-1} at high coverage. This value is comparable with other porous frameworks candidate for CO_2 capture such as NaX from zeolite family,[36] functionalized conjugated nanoporous polymers (CMP),[37] and Cu-BTC from MOF family[36] and thus could be considered within an ideal range to balance the favourable CO_2-framework interaction and energy demand for material regeneration. The favourable interaction between the Azo-COP-2 framework and the CO_2 molecules could then be attributed to the presence of the azobenzene moiety and was also previously observed in azo-based MOF.[32, 38] In conclusion, through various characterizations and data analysis, we have shown that the Azo-COP-2 has been successfully synthesized for this study.

Due to the existence of the azobenzene moiety which is responsive towards light, we are also interested in investigating the photo-switching property in Azo-COP-2 particles. Investigation on the potential of azobenzene functionality in this material has been previously attempted.[10] However, differing from previous investigation in Azo-COP-2, we are more focused on the potential application of Azo-COP-2 as low-energy CO_2 adsorbent that uses UV light as one of the main sources for material regeneration.[11] This then also complements the main application of the Azo-COP-2 as a highly-selective adsorbent for post-combustion CO_2 capture application.

The CO_2 light-responsive property of Azo-COP-2 was then investigated both in the static and dynamic condition and the result is presented in **Figure 4**. In both conditions, we then compared the CO_2 uptake of Azo-COP-2 between the normal and the UV-irradiated condition. During the static experiment, we observed that the CO_2 adsorption capacity of Azo-COP-2 significantly decreased from 2.12 mmol g^{-1} to be around 1.66 mmol g^{-1} at 273 K and from 1.28 mmol g^{-1} to be around 1.05 mmol g^{-1} at 298 K once exposed to UV-light. This decrease of CO_2 uptake was then found to be around 22% and 16% at 273 K and 298 K, respectively, compared with the values at the normal condition. The reduction of CO_2 uptake was not only observed in static condition but also in dynamic condition. As can also be seen, during the dynamic photo-switching experiment, when the UV light was on, the CO_2 uptake of Azo-COP-2 could instantaneously decrease to the value corresponded in the static condition experiment. This then shows the consistency between the dynamic and static conditions as previously observed in azobenzene-containing MOFs.[12, 38, 39]
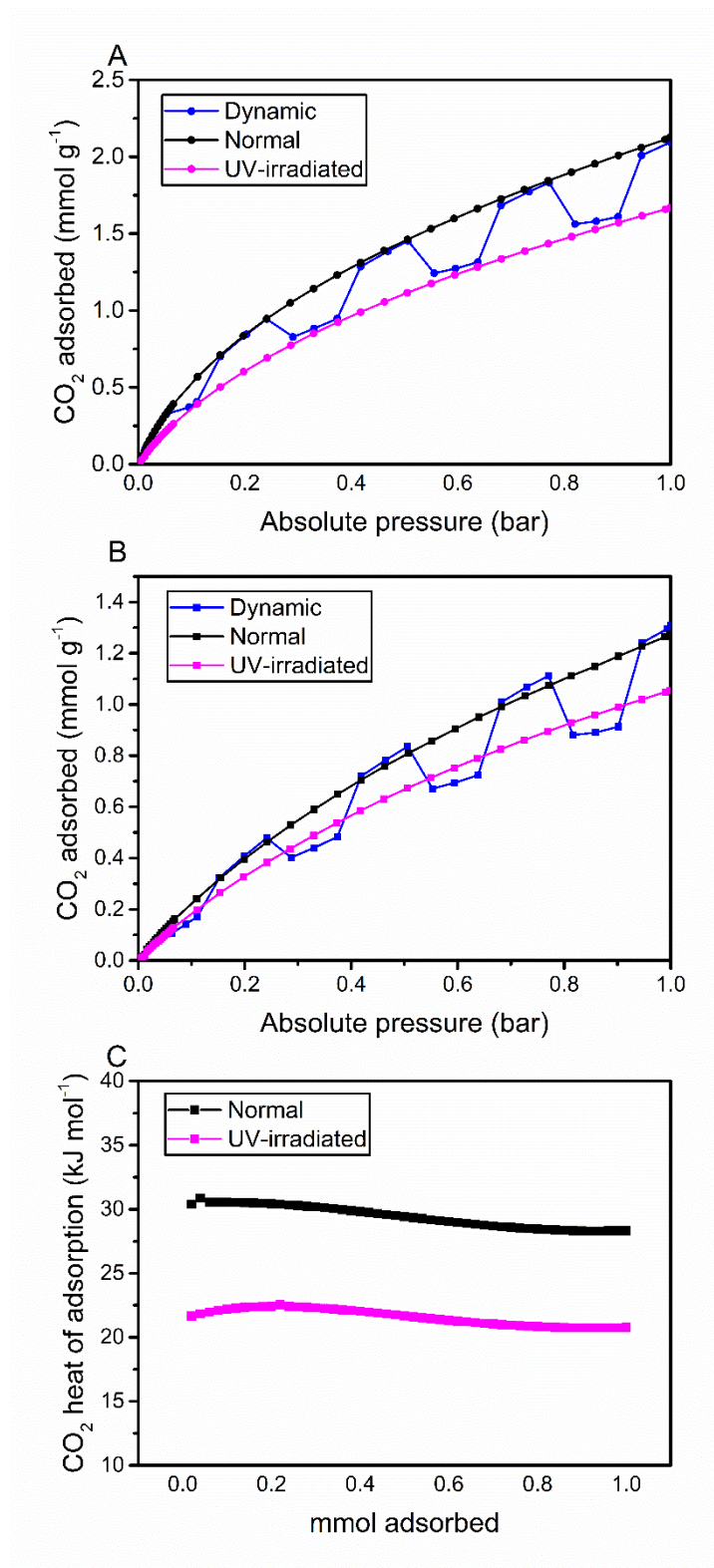
Figure 4. CO₂ photo-switching experiment of Azo-COP-2 at 273 K (A) and 298 K (B) and its CO₂ heat of adsorption (C)

In azobenzene-containing compounds, the light-responsive property is attributed to the photo-isomerization of the azobenzene moiety that isomerizes from its thermodynamically stable *trans*-state to less stable *cis*-state. Meanwhile, in Azo-COP-2 the azobenzene isomerization process might be hindered because of the rigid three-dimensional structure of the framework. As a result of this inhibited isomerization, the CO_2 adsorbed could be instantaneously released when the UV light was switched on resulting in excellent agreement of the CO_2 uptake in the static and dynamic experiment. This phenomenon was also previously observed in generation-3 light-responsive MOFs where hindered isomerization of the azobenzene framework also leads to instantaneous release of adsorbed CO_2 from the framework.[12, 33, 39] This is also evident from the CO_2 heat of adsorption profile of Azo-COP-2 between its normal and UV-irradiated condition. As can be seen in **Figure 4 (C)**, under UV light irradiation, the Q_{st} of Azo-COP-2 was found to be around 20 kJ mol^{-1} which is about 30% lower compared with the Q_{st} in normal condition which was around 28 kJ mol^{-1}. This then indicates that under UV-light irradiation, the Azo-COP-2 framework that is experiencing inhibited isomerization has lower affinity towards CO_2 than in normal condition resulting in instantaneous release of CO_2 as also previously observed in JUC-62 MOF.[33]

Although the CO_2 uptake decrease in the presence of UV-light was not as high as some previously reported light-responsive MOFs which could fall in the range between 33-50 %,[34, 39, 40] to the best of our knowledge, this is the first instance of dynamic CO_2 photo-switching observed in nanoporous polymers since previous investigations were limited to highly-crystalline MOFs. This then shows that in the amorphous porous polymers with excellent CO_2/N_2 selectivity and contain photo-active functionality like Azo-COP-2, the restricted movement of the photo-active framework could be further utilized to design a photo-responsive CO_2 adsorbent applicable for a low-energy and more sustainable post-combustion CO_2 capture. This is because such an adsorbent could exploit abundant UV light as a sustainable energy source to release the adsorbed CO_2 from its framework during the regeneration process. In practice, this could be accomplished by concentrating UV light on a quartz-column which is packed with UV-responsive adsorbent.[11] However, more research is still required to make this advanced process feasible and thus enabling them to replace the current post-combustion CO_2 capture and separation that still rely on non-sustainable resources during their regeneration process.

3.2 Azo-COP-2 Mixed Matrix Membranes (MMMs)

Apart from investigating the novel feature of Azo-COP-2 as a UV light-responsive adsorbent for low-energy CO_2 capture, we also expanded the investigation to study the potential of Azo-COP-2 as a porous filler in mixed matrix membranes (MMMs). This is based on our previous investigations in azobenzene-containing MOF MMMs showing the possibility to improve the membrane performance for CO_2/N_2 separation[30, 32] and the previous investigation on Azo-COP-2 has also shown satisfactory performance of the material for having high CO_2/N_2 selectivity.[5] Therefore, this study also aims to broaden the applicability of Azo-COP-2 in post-combustion CO_2 separation field not only as a candidate for low-energy adsorbent but can also be beneficial in a continuous membrane-based process.

Three different polymers were then chosen in this study to fabricate the MMMs: Matrimid, polysulfone and PIM-1. The particle loading was varied from 5 to 15 wt% for each type of polymer. During the MMMs fabrication, it was observed that the highest particle loading that could be obtained was 15wt% for all the three polymers. Higher particle loading led to structural brittleness of the resulting membranes and thus rendered them not suitable for testing. This phenomenon is quite common in composite membrane fabrication, in particular if the particle size of the filler is not small enough to be evenly distributed across the membrane. In our case, higher particle agglomeration and uneven distribution might cause this phenomenon as we observed the tendency of particle sedimentation and agglomeration when preparing the membrane dope solution. Apart from structural brittleness, this phenomenon could also lead to the formation of non-selective voids and a defective membrane. Because of this consideration, the particle loading in all MMMs was limited to 15 wt%. The resulting MMMs were then characterized using FTIR and SEM.

From the FTIR spectra (Figure S1), the presence of Azo-COP-2 in all the polymer matrices could be confirmed. First, although relatively weak, the stretching vibration of C=C from azo-phenyl group that occurs around 1600 cm^{-1} could be observed in all the three different MMMs used in this study. This value is slightly shifted in polysulfone-based MMMs which might be caused by the particle-polymer interaction. As previously explained, the relatively weak FTIR signal in the MMMs might be caused by the symmetrically substituted *trans*-state azo compounds resulting in weaker transmittance in FTIR spectrum.[35] The indication of Azo-COP-2 is more pronounced by the additional peak appearing at around 808 cm^{-1} which can be assigned to N=N bonding in

azobenzene. In case of both Matrimid and PIM-1, the additional peak leads to peak broadening of the adjacent peak. However, the signal could not be clearly observed in polysulfone-based MMMs, which might be caused by some overlapping with the polysulfone peaks. These results then give an indication of the existence of the Azo-COP-2 inside the polymeric matrices.

The presence and impact of the Azo-COP-2 incorporation on the microstructure of the three different polymers were then investigated through SEM imaging of the MMMs cross-section and the result is presented in **Figure 5**. Compared with the bare polymeric membranes (Figure S2), it could be seen that the microstructure of the MMMs are less continuous because of the presence of Azo-COP-2. This condition was more pronounced with MMMs at higher particle loading. At the macroscale level, this resulted in all the MMMs becoming more brittle and were prone to cracking during handling. Therefore, the particle loading in this study was capped at 15 wt%. From the SEM result, it could also be observed that the Azo-COP-2 particles could be uniformly dispersed inside the polymeric matrix although some particle agglomerations leading to the formation of particle aggregates could still be observed, in particular with MMMs with the highest particle loading. In addition, we also did not observe any obvious defects at the Azo-COP-2 – polymer interface for all the polymers used in this study. This might be attributed to the entirely organic framework of Azo-COP-2 which enables it to build good interaction at the interface with the polymer matrices.
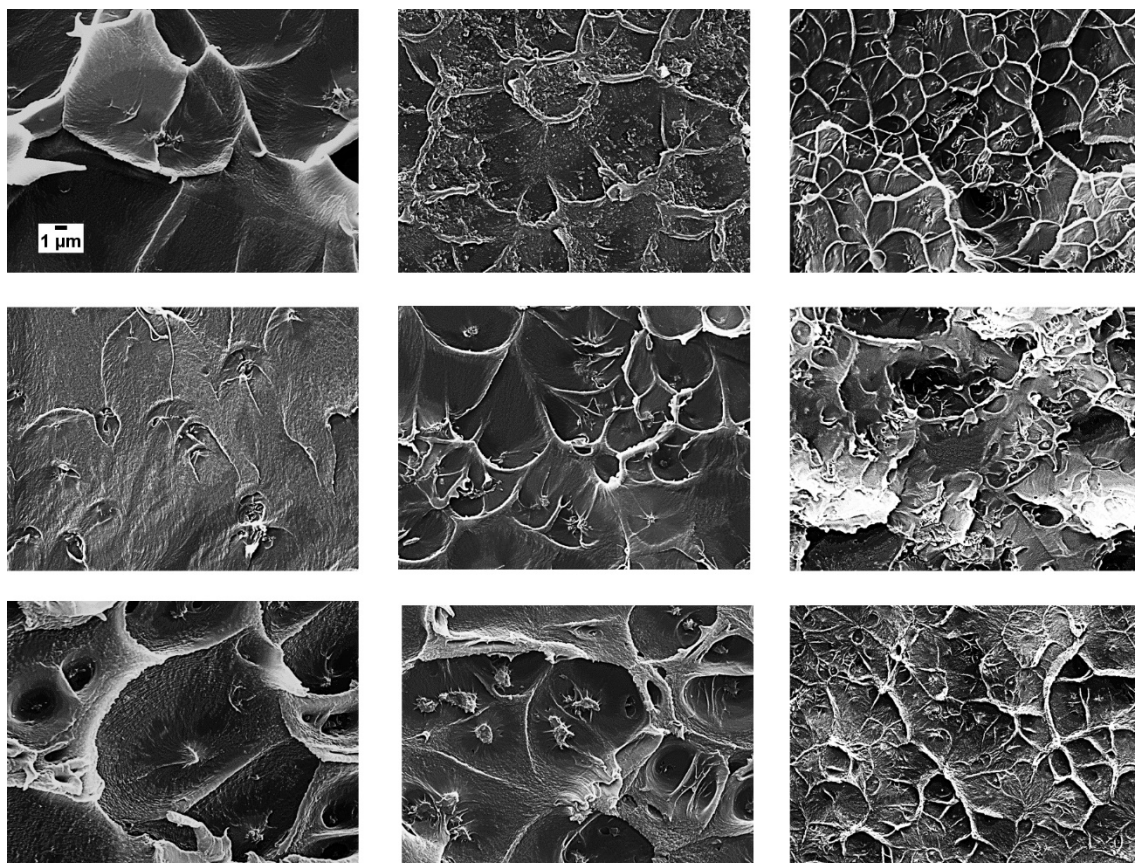
Figure 5. SEM micrographs of the Azo-COP-2 MMM. Top to bottom: Matrimid-based, polysulfone-based, and PIM-1-based MMMs. Left to right: 5 wt%, 10 wt% and 15 wt% particle loading.

The performance of the resulting Azo-COP-2 based MMMs were then evaluated for CO_2/N_2 separation. The result for the membranes permeability and selectivity is presented in **Figure 6**.
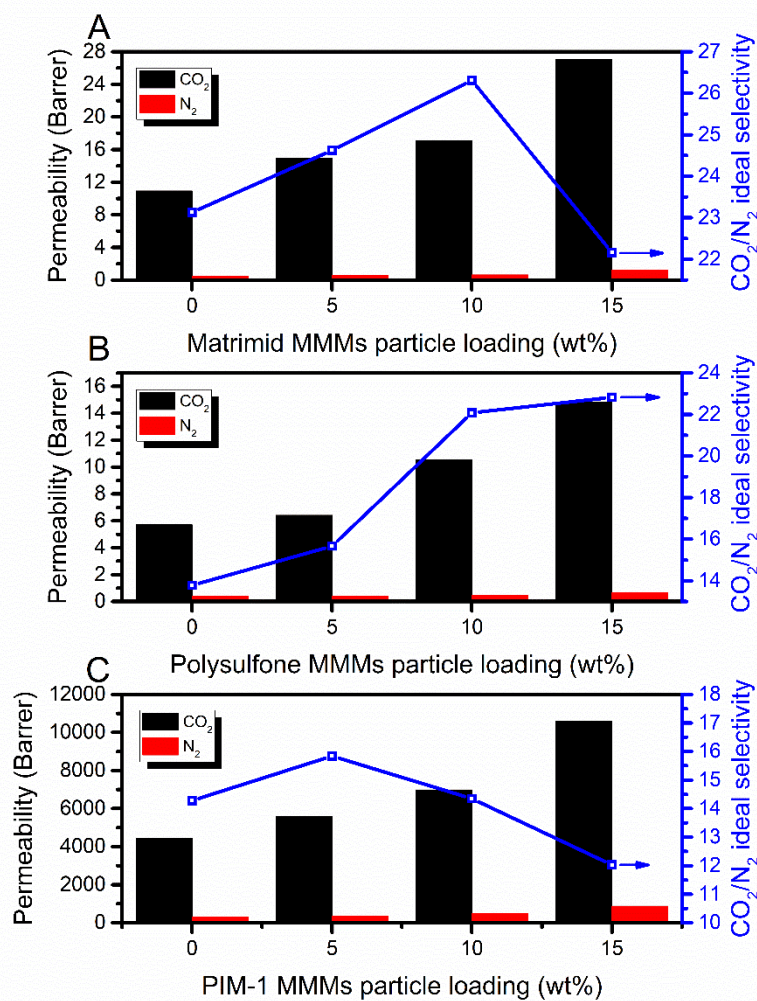
Figure 6. CO_2/N_2 gas separation performance of Matrimid (A), polysulfone (B) and PIM-1 (C) mixed matrix membranes

First of all, it could be seen for Matrimid-based MMMs that the CO_2 permeability could be increased at higher loading. The CO_2 permeability of bare Matrimid was found to be around 10 Barrer which is close to other reports for Matrimid membrane.[41-43] This value could be increased to 14.9 Barrer and 17.1 Barrer for 5 wt% and 10 wt% MMMs, respectively. As the Azo-COP-2 loading reached to 15 wt%, CO_2 permeability further increased to 27.1 Barrer, which is 171% higher than the CO_2 permeability of pure Matrimid membrane. The incorporated Azo-COP-2 nanoparticles might enhance the free volume in the membrane resulting in higher membrane permeability [22]. Meanwhile for the membrane selectivity, the bare Matrimid membrane CO_2/N_2 selectivity was found to be around 23 and comparable with other findings.[44, 45] It slightly increased to 24.6 and 26.3 at 5 wt% and 10wt% loading, respectively. A slightly lower CO_2/N_2 selectivity of 22.2

17

was observed upon 15 wt% Azo-COP-2 loading which is comparable with the selectivity of the bare Matrimid. Higher loading of particles may result in the generation of non-selective interfacial defects that is due to the poor adhesion at the interface of filler and polymer which leads to a lower CO_2/N_2 selectivity. The presence of this non-selective void might contribute in enhancing both CO_2 and N_2 permeability and thus reducing the CO_2/N_2 ideal selectivity.

The second polymer investigated in this study was polysulfone. Polysulfone is used as a membrane material for gas separation because of its resistance to chemicals and high temperatures and also commercial availability.[46, 47] As in Matrimid, the CO_2 permeability of the polysulfone-based MMMs could be increased at higher particle loading, the permeability of CO_2 increases from 5.7 for the bare membrane to be around 14.8 Barrer for the MMMs with the highest loading. The additional transport pathways provided by Azo-COP-2 are likely to account for the improvement in permeability. Meanwhile, the selectivity for the bare Polysulfone membrane was found to be around 13.7. Although this value differs from some other findings in polysulfone based membrane, it is still comparable with other findings when THF was used as one of the solvents to prepare the membrane.[48] Interestingly, differing from Matrimid, the ideal selectivity of the polysulfone-based MMMs could be continuously increased to be 15.7, 22.1 and 22.8 for 5 wt%, 10 wt% and 15 wt% particle loading, respectively. This indicates the absence of non-selective voids at the particle-polymer interface as previously observed in Matrimid. Once the good polymer-particle interface could be established, the N_2-phobic and CO_2-philic property of the azo group in Azo-COP-2 could then contribute to enhancing CO_2/N_2 selectivity in the MMMs.

Lastly, we also studied the MMMs by using PIM-1 as the polymer matrix. PIM-1 is a new type of high free volume polymers with potential applications in gas storage and membrane for gas separation because of its high permeability and moderate selectivity.[49] In this study, it is expected that the incorporation of Azo-COP-2 into PIM-1 could improve the separation performance of PIM-1. Firstly, it was observed that the CO_2 permeability for the bare PIM-1 membrane is around 4500 Barrer with selectivity around 14. This value is comparable with other findings in PIM-1 membrane.[50, 51] Upon incorporation of Azo-COP-2, the permeability could be further increased to be around 5500, 7000 and 10500 Barrer for 5, 10 and 15 wt% loading, respectively. However the selectivity did not likewise increase with loading. The selectivity for 5 wt% PIM-1 MMM could be slightly increased to be around 16. However, at higher particle loading, the selectivity decreased

and its value was comparable with the bare PIM-1. The selectivity was found to be around 14.3 and 12 for 10 wt% and 15 wt% particle loading, respectively. This phenomenon might be attributed to the creation of non-selective voids at the particle-polymer interface resulting in higher gas permeability but lower selectivity. As can also be seen from SEM micrographs, the particle agglomerations for PIM-1 at higher particle loading was more serious than at lower loading which could lead to the building of the non-selective voids.

Diffusivity and solubility coefficient are then calculated to gain a better understanding of the gas transport in the MMMs. The result is presented in **Figure 7 (A) and (B)** both for diffusion and solubility calculation, respectively. From **Figure 7 (A)**, a simultaneous enhancement of diffusivity values for CO_2 and N_2 for MMMs could be observed. This could be attributed to the additional free volume by incorporating Azo-COP-2 in any polymer matrix [23]. However, it could also be seen that the diffusivity selectivity of all the MMMs in this study remains almost constant. This then indicates that the additional pathways built from the Azo-COP-2 is not particularly selective towards CO_2. Apart from the similarities in CO_2 and N_2 kinetic diameter, this could also be attributed by the presence of the non-selective void at the particle-polymer interface as indicated by the slight decrease in diffusivity selectivity for MMMs at higher loading.
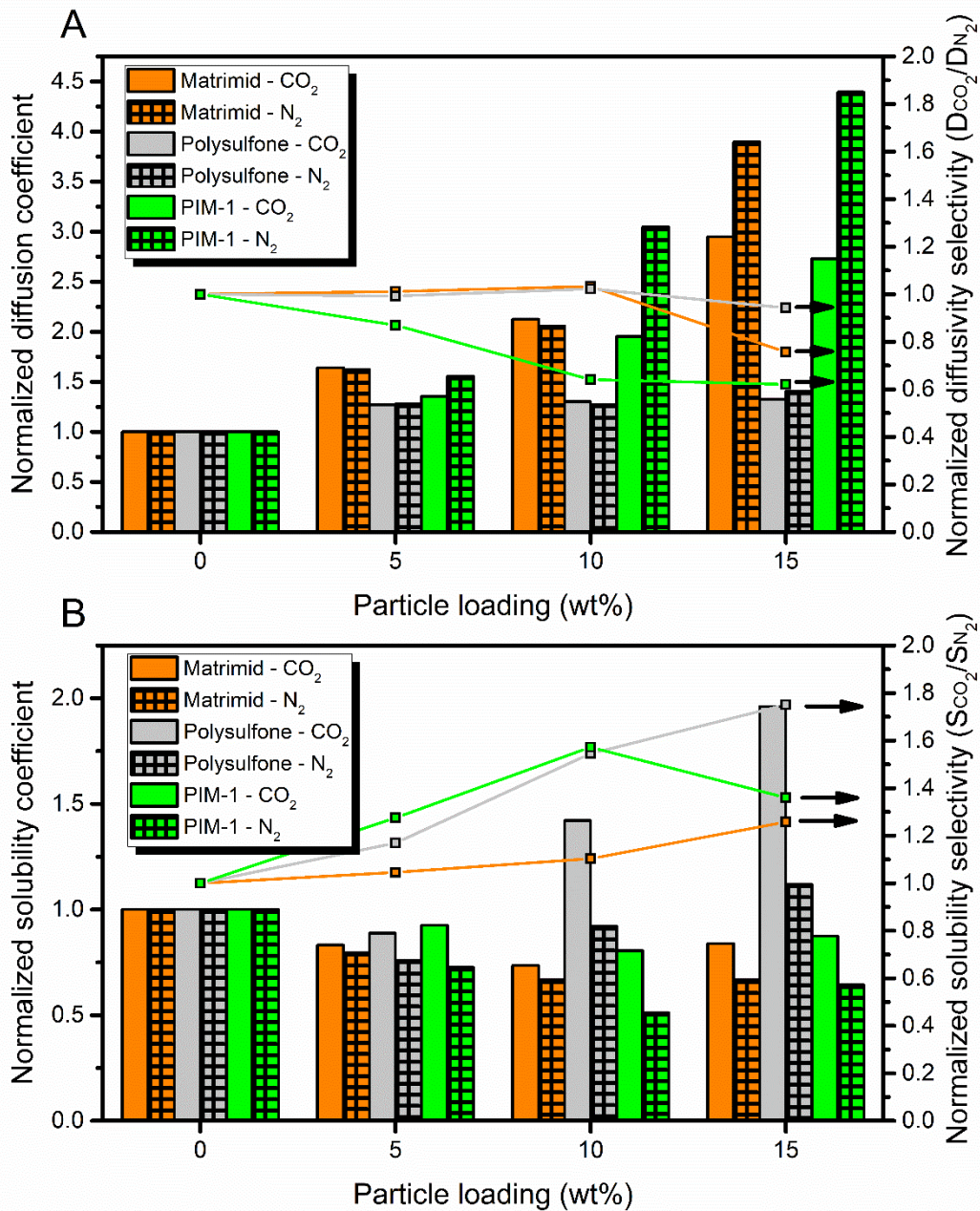
Figure 7. Normalized diffusivity (A) and solubility (B) coefficient and selectivity for mixed matrix membranes used in this study

A different trend, however, was observed for solubility coefficient of the MMMs as can be seen in **Figure 7 (B)**. First, it was observed that there was a decreasing trend for both CO_2 and N_2 solubility that could be caused by lower sorption volume provided by the MMMs as previously observed in other MMMs.[52, 53] Despite this, the solubility selectivity could be increased for the MMMs used in this study. Since solubility is related to a

thermodynamic property of the membranes,[46] this then highlights the advantage of incorporating Azo-COP-2 inside the membranes since it contributes to alter the thermodynamic behaviour of the resulting MMMs to be more favourable towards CO_2 rather than N_2.

However, it should be noted that in order to enhance the overall MMMs selectivity, the increase in solubility selectivity must be accompanied by relatively constant diffusivity selectivity. Although this case could be observed for most of the MMMs used in this study, a couple of non-ideal scenarios did also occur. For instance, as observed in 10 wt% PIM-1 and 15 wt% Matrimid MMMs, although the solubility selectivity could be increased, this was also accompanied by significant reduction in the diffusivity selectivity resulting in bare enhancement in overall selectivity. Furthermore, in case of PIM-1, once the particle loading was further increased to 15 wt%, the interaction between Azo-COP-2 and the PIM-1 might not be well established resulting in reduction of both diffusivity and solubility selectivity. In these cases, the Azo-COP-2 was then no longer able to significantly enhance the separation performance of the polymer and thus only contributes in enhancing gas transport across the membrane. Therefore, the defects at the polymer-particles interface must be avoided to obtain an ideal MMM behaviour since the presence of such defects contribute in disabling the molecular sieving aspect of the resulting MMMs resulting in lower selectivity. This is the ideal scenario which was observed on Polysuflone-based MMMs used in this study. As can be seen, both permeability and selectivity of the MMMs could be increased as the particle Azo-COP-2 particle loading was increased and thus indicating the absence of polymer-particle interfacial defects. Two things then could explain this behaviour which was not observed in Matrimid and PIM-1 based MMMs. First, this could be attributed to the hydrophobic interaction between the azobenzene functionality and polysulfone since both of them are inherently hydrophobic.[54-56] A similar scenario was also previously observed with zeolite-polysulfone MMMs.[57] Second, this could be related to polymer chain flexibility. Since polysulfone has a lower glass transition temperature (Tg) than Matrimid and PIM-1,[58-60] it should have a more flexible polymer chain. This flexibility could then contribute in establishing a better interaction with the particles and thus avoiding the building up of defective sites at the polymer-particle interface. This could happen particularly during the membrane drying period at elevated temperature.

Finally, we also evaluate the performance of the MMMs fabricated in this study with other COF-based MMMs for CO_2/N_2 separation. The result is presented in **Figure 8 (A) and**

(B) showing the membrane performance against the 2008 Robeson Upper Bound[61] and their relative performance improvement from the bare polymeric membranes, respectively.
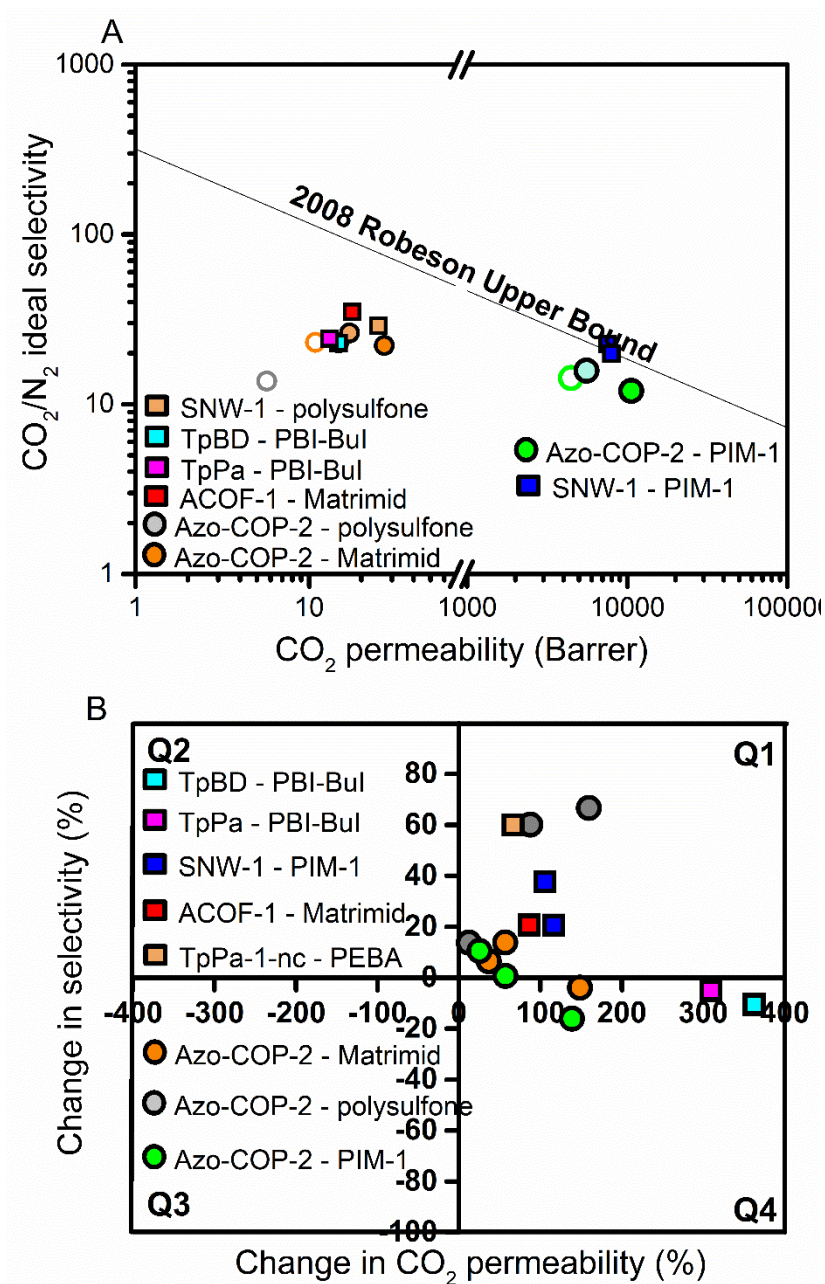

Figure 8. COF mixed matrix membranes for CO$_2$/N$_2$ gas separation performance against 2008 Robeson Upper Bound (A) and its corresponding permeability and selectivity improvement (B)

First of all, it could be seen that from the MMMs used in this study, the Azo-COP-2 – PIM-1 composite membranes showed the most satisfying performance regarding the permeability-selectivity trade-off. This phenomenon is expected since although both Matrimid and polysulfone have relatively high selectivity, their permeability is relatively low. Therefore, higher particle loading is necessary to further increase the polymeric membrane permeability. However, this approach does pose a risk to make the membrane more defective and eventually sacrificing the selectivity as what we observed with the 15 wt% Azo-COP-2 – Matrimid MMM. Meanwhile the CO_2 permeability in PIM-1 is relatively high with a moderate selectivity. Thus, incorporation of nanoporous polymers at low loading could be expected to significantly improve the membrane permeability without sacrificing the selectivity. As observed in this study, although at the highest loading the Azo-COP-2 was barely able to significantly improve the composite membrane selectivity, they could still enhance the composite membrane permeability resulting in the composite membrane performance to be close to the 2008 Robeson Upper Bound. A similar condition was also observed in SNW-1 nanoporous polymers when incorporation of the particles into PIM-1 could push the composite membrane performance to surpass the 2008 Robeson Upper Bound.[28]

The membranes performance could also be further evaluated based on the permeability and selectivity improvement. As can be seen in **Figure 8 (B)**, for Azo-COP-2 based MMMs, the permeability improvement was found to be in the range of 140-160% at the highest loading which is slightly higher than most of the COF-based MMMs used for CO_2/N_2 separation. Thus, Azo-COP-2 is beneficial in improving membrane productivity. Meanwhile for gas selectivity, Azo-COP-2 was able to improve this property up to 67% in the most ideal scenario where polysulfone was used as the polymer matrix. In this case, both MMMs permeability and selectivity could be simultaneously improved resulting in enhancement of both membrane productivity and effectiveness. In this ideal scenario, the polysulfone-based MMMs could then move towards the upper right corner of the Q1 region where both membrane permeability and selectivity could be improved simultaneously. Together with Azo-COP-2, ACOF-1,[62] SNW-1[28] and TpPA-1-nc[63] nanoporous polymers are reportedly able to push the bare polymeric membranes into this region. Apart from better interaction between the polymer and the particles, this phenomenon might also be caused by the nitrogen-rich framework possessed by the nanoporous polymers which imparts satisfactory CO_2/N_2 ideal selectivity as an adsorbent. For instance, TpPA-1 nanoporous polymers are rich in amide groups which were reported to have CO_2/N_2 selectivity at around 70[63]. Meanwhile for Matrimid and PIM-1

based MMMs, non-ideal behaviour was observed at higher particle loading resulting in loss in membrane selectivity and the resulting MMMs fall between the Q1 and Q4.

4 Conclusions

In this study, Azo-COP-2 has been successfully synthesized and fully characterized using different techniques including PXRD, FTIR, N_2 physisorption and CO_2 adsorption. Since Azo-COP-2 is built from azobenzene framework, a novel investigation was then conducted on this material to study its potential for low-energy CO_2 adsorbent through the CO_2 photo-switching adsorption both in static and dynamic condition. It was observed that Azo-COP-2 could experience a highly efficient CO_2 photo-switching with up to 25% instantaneous release of adsorbed CO_2 once irradiated with UV light. To the best of our knowledge, this is the first investigation on CO_2 dynamic photo-switching on nanoporous polymers which enables them to be applied in a low-energy CO_2 capture.

As an advanced CO_2 adsorbent with superior CO_2/N_2 separation and light-responsive property, a further investigation was made to incorporate Azo-COP-2 as nanoporous filler in polymer matrix through mixed matrix membranes (MMMs) fabrication for CO_2/N_2 separation. Three different polymers were used in this study: Matrimid, polysulfone and PIM-1. In all cases, MMMs had higher CO_2 permeability compared with their bare polymers indicating the beneficial impact of incorporating Azo-COP-2 to enhance the CO_2 transport. Within the range of particle loading used in this study, the polysulfone-based MMMs showed an increasing trend on both permeability and selectivity. The CO_2 permeability and CO_2/N_2 ideal selectivity increased from 5.7 Barrer and 13.8, respectively, for the bare Polysulfone membrane to 14.8 Barrer and 22.8, respectively, for MMM with 15 wt% particle loading. Meanwhile in terms of permeability-selectivity trade-off, PIM-1 based MMMs showed the best performance. Although the CO_2/N_2 ideal selectivity was relatively constant, a significant improvement in CO_2 permeability pushed the PIM-1 based MMMs performance for getting close to the 2008 Robeson Upper Bound.

In conclusion, this study has successfully advanced the application of Azo-COP-2 nanoporous polymer. The CO_2 photo-responsive nature of Azo-COP-2 makes them a promising potential material for advanced low-energy CO_2 separation. Meanwhile, Azo-COP-2 also acts as a good filler candidate for mixed matrix membranes which may be applicable for post combustion CO_2 capture

Acknowledgements

Supporting Information

FTIR spectra of Matrimid (A), polysulfone (B) and PIM-1 (C) based mixed matrix membranes; Cross section SEM micrographs of pure polymer matrices; Summary of diffusivity and solubility for Azo-COP-2/Matrimid, Azo-COP-2/Polysulfone, Azo-COP-2/PIM-1 MMMs.

Data Repository

The raw data for all figures in this manuscript, as well as the full resolution SEM micrographs, are available from the open repository https://doi.org/10.5281/zenodo.1469797

References

1.	Thommes, M.; Kaneko, K.; Neimark, A. V.; Olivier, J. P.; Rodriguez-Reinoso, F.; Rouquerol, J.; Sing, K. S., Physisorption of gases, with special reference to the evaluation of surface area and pore size distribution (IUPAC Technical Report). *Pure Appl. Chem.* **2015,** 87, (9-10), 1051-1069.

2.	James, S. L., Metal-organic frameworks. *Chem. Soc. Rev.* **2003,** 32, (5), 276-288.

3.	Feng, X.; Ding, X.; Jiang, D., Covalent organic frameworks. *Chem. Soc. Rev.* **2012,** 41, (18), 6010-6022.

4.	McKeown, N. B.; Budd, P. M., Polymers of intrinsic microporosity (PIMs): organic materials for membrane separations, heterogeneous catalysis and hydrogen storage. *Chem. Soc. Rev.* **2006,** 35, (8), 675-683.

5.	Patel, H. A.; Je, S. H.; Park, J.; Chen, D. P.; Jung, Y.; Yavuz, C. T.; Coskun, A., Unprecedented high-temperature CO2 selectivity in N2-phobic nanoporous covalent organic polymers. *Nat. Commun.* **2013,** 4, 1357.

6.	Jiang, Q.; Huang, H.; Tang, Y.; Zhang, Y.; Zhong, C., Highly Porous Covalent Triazine Frameworks for Reversible Iodine Capture and Efficient Removal of Dye. *Ind. Eng. Chem. Res.* **2018,** 57, (44), 15114-15121.

7.	Huang, N.; Chen, X.; Krishna, R.; Jiang, D., Two‐dimensional covalent organic frameworks for carbon dioxide capture through channel‐wall functionalization. *Angew. Chem. Int. Ed.* **2015,** 54, (10), 2986-2990.

8.	Fang, Q.; Gu, S.; Zheng, J.; Zhuang, Z.; Qiu, S.; Yan, Y., 3D microporous base‐functionalized covalent organic frameworks for size‐selective catalysis. *Angew. Chem.* **2014,** 126, (11), 2922-2926.

9.	Mahajan, R.; Koros, W. J., Factors controlling successful formation of mixed-matrix gas separation materials. *Ind. Eng. Chem. Res.* **2000,** 39, (8), 2692-2696.

10.	Patel, H. A.; Je, S. H.; Park, J.; Jung, Y.; Coskun, A.; Yavuz, C. T., Directing the Structural Features of N2‐Phobic Nanoporous Covalent Organic Polymers for CO2 Capture and Separation. *Chem. Eur. J.* **2014,** 20, (3), 772-780.

11.	Ladewig, B. P.; Lyndon, R.; Hill, M. R., The carbon sponge: squeezing out captured carbon dioxide. *Carbon Manag.* **2014,** 5, (1), 9-11.

12.	Lyndon, R.; Konstas, K.; Ladewig, B. P.; Southon, P. D.; Kepert, P. C. J.; Hill, M. R., Dynamic Photo‐Switching in Metal−Organic Frameworks as a Route to Low‐Energy Carbon Dioxide Capture and Release. *Angew. Chem. Int. Ed.* **2013,** 52, (13), 3695-3698.

13.	Collet, G.; Lathion, T. e.; Besnard, C. l.; Piguet, C.; Petoud, S. p., On-Demand Degradation of Metal–Organic Framework Based on Photocleavable Dianthracene-Based Ligand. *J. Am. Chem. Soc* **2018,** 140, (34), 10820-10828.

14.	Zhang, J.; Wang, L.; Li, N.; Liu, J.; Zhang, W.; Zhang, Z.; Zhou, N.; Zhu, X., A novel azobenzene covalent organic framework. *CrystEngComm* **2014,** 16, (29), 6547-6551.

15.	Liu, C.; Zhang, W.; Zeng, Q.; Lei, S., A Photoresponsive Surface Covalent Organic Framework: Surface‐Confined Synthesis, Isomerization, and Controlled Guest Capture and Release. *Chem. Eur. J.* **2016,** 22, (20), 6768-6773.

16.	Baroncini, M.; d'Agostino, S.; Bergamini, G.; Ceroni, P.; Comotti, A.; Sozzani, P.; Bassanetti, I.; Grepioni, F.; Hernandez, T. M.; Silvi, S., Photoinduced reversible switching of porosity in molecular crystals based on star-shaped azobenzene tetramers. *Nat. Chem.* **2015,** 7, (8), 634-640.

17.	Zhu, Y.; Zhang, W., Reversible tuning of pore size and CO 2 adsorption in azobenzene functionalized porous organic polymers. *Chem. Sci.* **2014,** 5, (12), 4957-4961.

18.   Rezakazemi, M.; Amooghin, A. E.; Montazer-Rahmati, M. M.; Ismail, A. F.; Matsuura, T., State-of-the-art membrane based CO2 separation using mixed matrix membranes (MMMs): an overview on current status and future directions. *Prog. Polym. Sci.* **2014,** 39, (5), 817-861.

19.   Sun, H.; Wang, T.; Xu, Y.; Gao, W.; Li, P.; Niu, Q. J., Fabrication of polyimide and functionalized multi-walled carbon nanotubes mixed matrix membranes by in-situ polymerization for CO2 separation. *Sep. Purif. Technol.* **2017,** 177, 327-336.

20.   Park, C. H.; Tocci, E.; Fontananova, E.; Bahattab, M. A.; Aljlil, S. A.; Drioli, E., Mixed matrix membranes containing functionalized multiwalled carbon nanotubes: Mesoscale simulation and experimental approach for optimizing dispersion. *J Memb Sci.* **2016,** 514, 195-209.

21.   Shen, G.; Zhao, J.; Guan, K.; Shen, J.; Jin, W., Highly efficient recovery of propane by mixed‐matrix membrane via embedding functionalized graphene oxide nanosheets into polydimethylsiloxane. *AlChE J.* **2017,** 63, (8), 3501-3510.

22.   Ahmad, N.; Leo, C.; Mohammad, A.; Ahmad, A., Modification of gas selective SAPO zeolites using imidazolium ionic liquid to develop polysulfone mixed matrix membrane for CO2 gas separation. *Microporous Mesoporous Mater.* **2017,** 244, 21-30.

23.   Ahmad, N.; Leo, C.; Mohammad, A.; Ahmad, A., Interfacial sealing and functionalization of polysulfone/SAPO-34 mixed matrix membrane using acetate-based ionic liquid in post-impregnation for CO2 capture. *Sep. Purif. Technol.* **2018,** 197, 439-448.

24.   Shahid, S.; Nijmeijer, K., Matrimid®/polysulfone blend mixed matrix membranes containing ZIF-8 nanoparticles for high pressure stability in natural gas separation. *Sep. Purif. Technol.* **2017,** 189, 90-100.

25.   Dechnik, J.; Sumby, C. J.; Janiak, C., Enhancing Mixed-Matrix Membrane Performance with Metal-Organic Framework Additives. *Cryst. Growth Des* **2017,** 17, 4467-4488.

26.   Hsieh, J. O.; Balkus, K. J.; Ferraris, J. P.; Musselman, I. H., MIL-53 frameworks in mixed-matrix membranes. *Microporous Mesoporous Mater.* **2014,** 196, 165-174.

27.   Hu, J.; Cai, H.; Ren, H.; Wei, Y.; Xu, Z.; Liu, H.; Hu, Y., Mixed-matrix membrane hollow fibers of Cu3 (BTC) 2 MOF and polyimide for gas separation and adsorption. *Ind. Eng. Chem. Res.* **2010,** 49, (24), 12605-12612.

28.   Wu, X.; Tian, Z.; Wang, S.; Peng, D.; Yang, L.; Wu, Y.; Xin, Q.; Wu, H.; Jiang, Z., Mixed matrix membranes comprising polymers of intrinsic microporosity and covalent organic framework for gas separation. *J Memb Sci.* **2017,** 528, 273-283.

29.   Gao, X.; Zou, X.; Ma, H.; Meng, S.; Zhu, G., Highly selective and permeable porous organic framework membrane for CO2 capture. *Adv. Mater.* **2014,** 26, (22), 3644-3648.

30.   Prasetya, N.; Teck, A. A.; Ladewig, B. P., Matrimid-JUC-62 and Matrimid-PCN-250 mixed matrix membranes displaying light-responsive gas separation and beneficial ageing characteristics for CO 2/N 2 separation. *Sci Rep.* **2018,** 8, (1), 2944.

31.   Cook, M.; Gaffney, P. R.; Peeva, L. G.; Livingston, A. G., Roll-to-roll dip coating of three different PIMs for Organic Solvent Nanofiltration. *J Memb Sci.* **2018,** 558, 52-63.

32.   Prasetya, N.; Ladewig, B. P., New Azo-DMOF-1 MOF as a Photoresponsive Low-Energy CO2 Adsorbent and Its Exceptional CO2/N2 Separation Performance in Mixed Matrix Membranes. *ACS Appl. Mater. Interfaces* **2018,** 10, (40), 34291-34301.

33.   Prasetya, N.; Ladewig, B. P., Dynamic photo-switching in light-responsive JUC-62 for CO 2 capture. *Sci Rep.* **2017,** 7, (1), s41598-017.

34.   Prasetya, N.; Donose, B. C.; Ladewig, B. P., A new and highly robust light-responsive Azo-UiO-66 for highly selective and low energy post-combustion CO 2 capture and its application in a mixed matrix membrane for CO 2/N 2 separation. *J. Mater. Chem. A* **2018,** 6, (34), 16390-16402.

35.   Larkin, P., General Outline and Strategies for IR and Raman Spectra Interpretation. In *Infrared and Raman spectroscopy: principles and spectral interpretation*, Elsevier: 2017.

36.   Xiang, S.; He, Y.; Zhang, Z.; Wu, H.; Zhou, W.; Krishna, R.; Chen, B., Microporous metal-organic framework with potential for carbon dioxide capture at ambient conditions. *Nat. Commun.* **2012,** 3, 954.

37.   Dawson, R.; Adams, D. J.; Cooper, A. I., Chemical tuning of CO 2 sorption in robust nanoporous organic polymers. *Chem. Sci.* **2011,** 2, (6), 1173-1177.

38.   Prasetya, N.; Ladewig, B. P., Dynamic photo-switching in light-responsive JUC-62 for CO 2 capture. *Sci Rep.* **2017,** 7, (1), 13355.

39.   Li, H.; Martinez, M. R.; Perry, Z.; Zhou, H.-C.; Falcaro, P.; Doblin, C.; Lim, S.; Hill, A.; Halstead, B.; Hill, M., A robust metal organic framework for dynamic light‑induced swing adsorption of carbon dioxide. *Chem. Eur. J.* **2016**.

40.   Park, J.; Yuan, D.; Pham, K. T.; Li, J.-R.; Yakovenko, A.; Zhou, H.-C., Reversible alteration of CO2 adsorption upon photochemical or thermal treatment in a metal–organic framework. *J. Am. Chem. Soc* **2011,** 134, (1), 99-102.

41.   Amooghin, A. E.; Omidkhah, M.; Kargari, A., Enhanced CO 2 transport properties of membranes by embedding nano-porous zeolite particles into Matrimid® 5218 matrix. *RSC Adv.* **2015,** 5, (12), 8552-8565.

42.   Perez, E. V.; Balkus, K. J.; Ferraris, J. P.; Musselman, I. H., Mixed-matrix membranes containing MOF-5 for gas separations. *J Memb Sci.* **2009,** 328, (1), 165-173.

43.   Dechnik, J.; Nuhnen, A.; Janiak, C., Mixed-Matrix Membranes of the Air-Stable MOF-5 Analogue [Co4 (µ4-O)(Me2pzba) 3] with a Mixed-Functional Pyrazolate-Carboxylate Linker for CO2/CH4 Separation. *Cryst. Growth Des.* **2017,** 17, (8), 4090-4099.

44.   Tessema, T. D. M.; Venna, S. R.; Dahe, G.; Hopkinson, D. P.; El-Kaderi, H. M.; Sekizkardes, A. K., Incorporation of benzimidazole linked polymers into Matrimid to yield mixed matrix membranes with enhanced CO2/N2 selectivity. *J Memb Sci.* **2018,** 554, 90-96.

45.   Wang, Y.; Hu, T.; Li, H.; Dong, G.; Wong, W.; Chen, V., Enhancing membrane permeability for CO2 capture through blending commodity polymers with selected PEO and PEO-PDMS copolymers and composite hollow fibres. *Energy Procedia* **2014,** 63, 202-209.

46.   Ahn, J.; Chung, W.-J.; Pinnau, I.; Guiver, M. D., Polysulfone/silica nanoparticle mixed-matrix membranes for gas separation. *J Memb Sci.* **2008,** 314, (1-2), 123-133.

47.   Zimmerman, C. M.; Singh, A.; Koros, W. J., Tailoring mixed matrix composite membranes for gas separations. *J Memb Sci.* **1997,** 137, (1-2), 145-154.

48.   Julian, H.; Sutrisna, P. D.; Hakim, A. N.; Harsono, H. O.; Hugo, Y. A.; Wenten, I. G., Nano-silica/polysulfone asymmetric mixed-matrix membranes (MMMs) with high CO2 permeance in the application of CO2/N2 separation. *Polym Plast Technol Eng* **2018**, 1-12.

49.   Budd, P. M.; Ghanem, B. S.; Makhseed, S.; McKeown, N. B.; Msayib, K. J.; Tattershall, C. E., Polymers of intrinsic microporosity (PIMs): robust, solution-processable, organic nanoporous materials. *Chem. Commun.* **2004,** (2), 230-231.

50.   Ahn, J.; Chung, W.-J.; Pinnau, I.; Song, J.; Du, N.; Robertson, G. P.; Guiver, M. D., Gas transport behavior of mixed-matrix membranes composed of silica nanoparticles in a polymer of intrinsic microporosity (PIM-1). *J Memb Sci.* **2010,** 346, (2), 280-287.

51.   Staiger, C. L.; Pas, S. J.; Hill, A. J.; Cornelius, C. J., Gas separation, free volume distribution, and physical aging of a highly microporous spirobisindane polymer. *Chem. Mater.* **2008,** 20, (8), 2606-2608.

52.   Zhao, D.; Ren, J.; Wang, Y.; Qiu, Y.; Li, H.; Hua, K.; Li, X.; Ji, J.; Deng, M., High CO2 separation performance of Pebax®/CNTs/GTA mixed matrix membranes. *J Memb Sci.* **2017,** 521, 104-113.

53.   Ghalei, B.; Sakurai, K.; Kinoshita, Y.; Wakimoto, K.; Isfahani, A. P.; Song, Q.; Doitomi, K.; Furukawa, S.; Hirao, H.; Kusuda, H., Enhanced selectivity in mixed matrix membranes for CO 2

capture through efficient dispersion of amine-functionalized MOF nanoparticles. *Nat. Energy.* **2017,** 2, (7), 17086.

54.   Aroon, M.; Ismail, A.; Matsuura, T.; Montazer-Rahmati, M., Performance studies of mixed matrix membranes for gas separation: a review. *Sep. Purif. Technol.* **2010,** 75, (3), 229-242.

55.   Sharma, N.; Purkait, M. K., Preparation of hydrophilic polysulfone membrane using polyacrylic acid with polyvinyl pyrrolidone. *J. Appl. Polym. Sci.* **2015,** 132, (22).

56.   Ishikawa, M.; Ohzono, T.; Yamaguchi, T.; Norikane, Y., Photo-enhanced Aqueous Solubilization of an Azo-compound. *Sci Rep.* **2017,** 7, (1), 6909.

57.   Gorgojo, P.; Uriel, S.; Téllez, C.; Coronas, J., Development of mixed matrix membranes based on zeolite Nu-6 (2) for gas separation. *Microporous Mesoporous Mater.* **2008,** 115, (1-2), 85-92.

58.   Baglay, R. R.; Roth, C. B., Local glass transition temperature T g (z) of polystyrene next to different polymers: Hard vs. soft confinement. *J. Chem. Phys* **2017,** 146, (20), 203307.

59.   Dorosti, F.; Omidkhah, M.; Abedini, R., Fabrication and characterization of Matrimid/MIL-53 mixed matrix membrane for CO2/CH4 separation. *Chem. Eng. Res. Des.* **2014,** 92, (11), 2439-2448.

60.   Li, P.; Chung, T.; Paul, D., Temperature dependence of gas sorption and permeation in PIM-1. *J Memb Sci.* **2014,** 450, 380-388.

61.   Robeson, L. M., The upper bound revisited. *J Memb Sci.* **2008,** 320, (1-2), 390-400.

62.   Shan, M.; Seoane, B.; Andres-Garcia, E.; Kapteijn, F.; Gascon, J., Mixed-matrix membranes containing an azine-linked covalent organic framework: Influence of the polymeric matrix on post-combustion CO 2-capture. *J Memb Sci.* **2018,** 549, 377-384.

63.   Zou, C.; Li, Q.; Hua, Y.; Zhou, B.; Duan, J.; Jin, W., Mechanical Synthesis of COF Nanosheet Cluster and Its Mixed Matrix Membrane for Efficient CO2 Removal. *ACS Appl. Mater. Interfaces* **2017,** 9, (34), 29093-29100.

Abstract Graphic